



# Artemia Cysts as dynamic biosorbent for efficient and fast uptake of lead ions from contaminated environments

S. Ziaei<sup>1</sup> · H. Ahmadzadeh<sup>1</sup> · Z. Es'haghi<sup>2</sup>

Received: 10 August 2021 / Revised: 2 November 2021 / Accepted: 5 December 2021  
© Islamic Azad University (IAU) 2021

## Abstract

This work proposes *Artemia* cysts as a dynamic and efficient biosorbent for the elimination of lead ion contaminants which can continuously produce new and multifold cysts as a sorbent in every cycle. Cyst of *Artemia* is composed of multiple layers covered with a porous surface and numerous functional groups that are capable of vigorous encapsulation of lead ions. Fourier transform infrared spectroscopy, scanning electron microscopy, energy-dispersive spectrometry and X-ray diffraction analyses were used to assess surface properties of the cyst. The most vital parameters in evaluating adsorption rate such as pH, contact time, initial concentration of lead ions and selectivity for uptake of the lead ions in the presence of high concentration of  $\text{Ca}^{2+}/\text{Mg}^{2+}/\text{Na}^{+}/\text{Cd}^{2+}/\text{Co}^{2+}/\text{Cu}^{2+}/\text{Mn}^{2+}/\text{Ni}^{2+}$  proved that rapid and robust biosorption occurred during these selectivity experiments. The most astounding result to appear from the data was that batch experiment showed the maximum uptake of 94.40% at pH 5.8 in less than 1 min with 50 mg L<sup>-1</sup> of initial concentration of lead ions. Equilibrium biosorption well fitted by Langmuir isotherm. The negative value of change in Gibbs free energy ( $\Delta G$ ) indicated the spontaneous adsorption of lead ion on the biosorbent. The enthalpy change indicated that an exothermic reaction was occurring during the biosorption process in which the  $\Delta H$  was -28.74 kJ mol<sup>-1</sup>. The results confirmed the efficient, simple and straight forward performance of *Artemia* cysts in purifying contaminated water from lead ions.

---

Editorial responsibility: Binbin Huang.

---

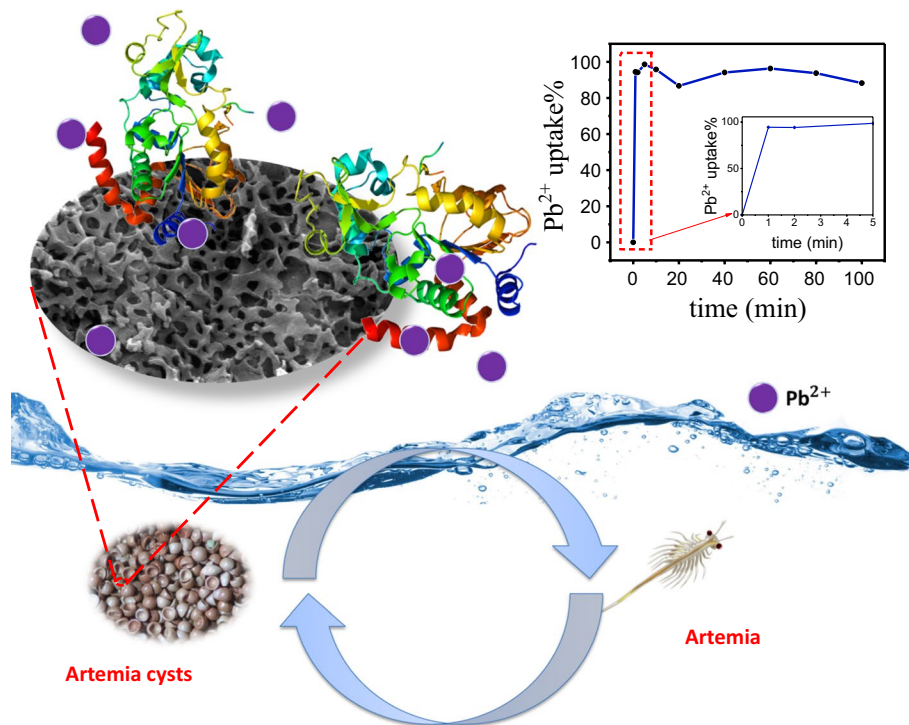
✉ H. Ahmadzadeh  
h.ahmadzadeh@um.ac.ir

<sup>1</sup> Department of Chemistry, Faculty of Science, Ferdowsi University of Mashhad, 9177948974 Mashhad, Iran

<sup>2</sup> Department of Chemistry, Payame Noor University, 19395-4697 Tehran, Iran



## Graphical abstract



**Keywords** Artemia cyst · Biosorption · Lead ions · Heavy metal ions, Langmuir isotherm, Freundlich isotherm

## Introduction

Water being an existential element that sustains life on earth undoubtedly gives rise to the cruciality of dealing with its contamination. Even trace amounts of heavy metal contaminating water impose a detrimental threat to human health (Bolisetty et al. 2019; Liang et al. 2019). Health experts in various regions of the world have reported illnesses such as nervous system failure, encephalopathy, skin faintness and lung cancer that were attributed to polluted water with trace amounts of arsenic (Sarode et al. 2019). Lead ions are among the most toxic and non-biodegradable heavy metals after arsenic found in water and waste water (Sarode et al. 2019). The main sources of lead pollution are manufacturing of batteries, industrial fuel, petroleum and plating industries resulting in irreversible affliction on living things. World Health Organization (WHO) in their 2019 report on lead poisoning through drinking water iterated that it can result in metabolic disorders, anemia, kidney failure, brain stroke, liver failure and cancer among other illnesses (Awual and Hasan 2019; WHO 2019; Kushwaha et al. 2020; Yılmaz et al. 2020).

Elimination of lead ions from water is being executed using various methods such as chemical precipitation,

coagulation, reverse osmosis, ion exchange and adsorption (Rao et al. 2007; Huang et al. 2011; Bowman et al. 2018; Vieira et al. 2018; Chen et al. 2019). Among these approaches, adsorption technique is considered to be the most efficient, owing it to its simple design, low-cost and eco-friendliness compared to other formal approaches (Cashin et al. 2018; Chatterjee et al. 2018; Li et al. 2018; Hannachi and Hafidh 2020). In spite of these advantages, scholarly research has been dedicated to developing these methods into cheaper and greener approaches, which has shifted their focus toward the investigation of natural adsorbents. Various biomaterials, such as waste of saffron flower (Khoshsang and Ghaffarinejad 2018), cucumber peel (Basu et al. 2017), egg shell (Meski et al. 2010), fruit peels (Mallampati et al. 2015; Turkmen Koc et al. 2020), cabbage waste (Hossain et al. 2014) and Taro (Saha et al. 2017), have been examined as sorbents to remove heavy metal ions. The functional groups on the surface of some adsorbents are a significant parameter that can contribute in eliminating heavy metal ions (Xu and Wang 2017; Wang and Zhuang 2017). Some studies based on proteins and their derivatives have been reported to use them as an excellent sorbent. Amino acids exist on proteins and their hybrid adsorbents constitute immense amounts of amide



bonds and carboxyl functional groups which can uptake heavy metal ions from wastewater (Koley et al. 2016a, b; Zhang et al. 2020).

In parallel with proteins, chitin and chitosan have been introduced as effective metal biosorbents from wastewater due to their amino and hydroxyl functional groups and unique properties such as biodegradability, high biosorption capacity, non-toxicity and efficient performance in aqueous solutions (Luo et al. 2015; Zhang et al. 2016; Sellaoui et al. 2017; Tolesa et al. 2019; Zia et al. 2020). These sorbents with free electron lone pairs on  $\text{-NH}_2$  and  $\text{-OH}$  functional groups can cross-link with heavy metal ions via chelation or ion-exchange mechanisms depending on their pH level. However, during the treatment process of wastewater, most biosorbents would be saturated with high salt ion concentrations, resulting in loss of chemical stability. Hence, researchers are persistently investigating the potential of adsorbents with sufficient capacity for intended ion adsorption in the presence of other competitive ions. Most of the materials that have substantial capacity for ion adsorption do not accomplish effective performance owing to the powerful competing affinity of ions. As is known, the general cations including  $\text{Na}^+$ ,  $\text{Ca}^{2+}$  and  $\text{Mg}^{2+}$  at high concentration are present in aqua environment of *Artemia* cyst and natural wastewaters. Thus, they influence lead ion biosorption.

*Artemia* (brine shrimp) are used as live food in fish cultivation and aquaculture. These species usually live in hypersaline lakes or oceans that are located in regions such as Europe, China, Japan, Iran and USA (Sorgeloos et al. 2001; Bergami et al. 2016; Le et al. 2019). Approximately 18,000 tons of *Artemia* have been used for fish feeding or annual cultivation demands all over the world (Brown 2012). Larvae emerge from *Artemia* cysts (A.C.) and would be collected for bait and discarded cyst shells would be disposed as wastes.

Several studies have been performed to use *Artemia* in ecotoxicology studies. Accordingly, cysts-based assays are cost effective, simple and suitable in routine experiments. A number of advantages can be considered including short-term nauplii hatchability, long-term mortality, high flexibility to hard environmental conditions, high fecundity and reproductive ability. At the same time, several disadvantages about its sensitivity toward a wide range of substances have been also presented (Libralato 2014; Kos et al. 2016).

Furthermore, *Artemia* cyst contains calcium, phosphor compounds, chitin, chitosan and 17 types of amino acids (Sugumar and Munuswamy 2006), whereby these structures are capable of seizing heavy metal ions through available amides and carboxyl groups. Additionally, chorion layer of cysts demonstrates satisfactory biocompatibility and eco-friendly properties amid harsh conditions. For instance, it indicates high adaptability with broad ranges of temperature and salinity, UV emission and oxygen-lacking environments

with protection of encysted embryos (Clegg et al. 1994; Wang et al. 2015; Song et al. 2022). Interestingly, the outer cuticular membrane of the cyst also illustrates inimitable heterogeneous three-dimensional structure of pores with micro-, medium- and macro-porous morphology in the range of micrometer to nanometer size which are suitable for the elimination of metal ions (Wang et al. 2018). More importantly, this layer acts as a filter and protects embryos from the penetration of molecules larger than carbon dioxide (MacRae 2016). This specification is considered a remarkable feature in eradicating heavy metals without damaging the embryos.

As mentioned earlier, the superior chemical stability of *Artemia* cysts in discordant conditions is regarded as an outstanding attribute of this species (Wang et al. 2010). The carboxyl and amide functional groups with three dimensional pore structures in cysts layer can strongly bind with heavy metal ions. In the same research, Wang et al., 2018 executed a progressive method and applied detached *Artemia* cyst shells and poured them into aqua solution which resulted in the elimination of lead ions (Wang et al. 2018).

On the contrary, the current research uses a singular stage of immediate release of the cysts directly into the polluted solution for the removal of toxic lead ions through an incessant sorption system of heavy metal contaminants. In particular specially, no report had previously seen to use *Artemia* cysts for contaminated water. Therefore, it is necessary to know this knowledge about biocompatible sorbent.

Depending upon water temperature, pH, salinity, etc., cysts will hatch in approximately 18–36 h and the nauplii are born. After hatching *Artemia*, the egg shells that uptake lead ions are floated and separated from nauplii. Normally, in the natural conditions it takes 3 to 6 weeks for brine shrimp to mature. Under optimal conditions, adult *Artemia* live for several months, and reproduce 50 to 200 eggs every 3–4 days. The surrounding shell protects embryo from the polluted elements. When conditions improve, the embryo resumes development, and the life cycle continues. So, automatically the cysts as sorbents will produce in regular time even with the entry of new contamination into the environment. Actually, this research suggests a novel, continuous system to use cysts for cleaning the contaminated waters that is able to uptake contaminated lead ions without extra cost. Also, cyst shells are waste with no economic value.

The introduction of this novel method integrates merits of simplicity, time optimization and affordability in addition to the reusability, good biodegradability, low cost, high efficiency and the possibility of metal recovery. The biosorbent was characterized using scanning electron microscopy (SEM), energy-dispersive spectrometry (EDS) and X-ray diffraction (XRD) and FT-IR techniques. Moreover, various effective influencers on biosorption were evaluated. Finally, the isotherms and thermodynamics parameter were



calculated. The date of this research was carried out in the Ferdowsi University in Mashhad, Iran (2019).

## Materials and methods

### Materials

Pb (NO<sub>3</sub>)<sub>2</sub> and HNO<sub>3</sub> from Merck (Darmstadt, Germany), Ca (NO<sub>3</sub>)<sub>2</sub> from BDH Laboratory Supplies (Poole, UK), Mg (NO<sub>3</sub>)<sub>2</sub> and NaOH from Riedel-de-Haen (Seelze, Germany) and Artemia cysts (A.C.) from Guar kavirarya (Tehran, Iran) were purchased. For the preparation of solutions, deionized (DI) water was used. All chemicals and reagents utilized in the experiment were of analytical grade and were applied without any alternative purification.

### Instruments

The concentration of Pb ions in the solution was determined with an atomic absorption spectrophotometer (Analytik Jena AG, 07,745 Jena, Germany). The surface morphology of the Artemia cyst before and after lead uptake was obtained using scanning electron microscopy (SEM) (TESCAN-XMU, Czech Republic) with an energy-dispersive X-ray spectrometer EDS analysis. The crystalline structure of the cyst before and after sorption of lead ions was recorded by X-ray diffraction (XRD) (Bruker D8, USA) advanced diffractometer with Cu K $\alpha$  radiation. A Fourier transform infrared (FT-IR) spectrometry (Thermo Nicolet Avatar 370, Pittsfield, USA) was used to characterize the chemical structure of the biosorbent samples. Inductively coupled plasma optical emission spectroscopy (ICP-OES) analysis was used to selectivity study.

### Treatment of the Artemia cysts

The A.C. were cleaned conducting the following steps. First, the A.C. (10 g) were added into a 300-mL water-ethanol mixture (50 w/w %) and stirred for 5 h to remove the salt and other residues. This procedure was repeated for 2–3 times. Then, A.C. were filtered and washed with deionized water. Finally, A.C. were heated and dried at 45 °C for 8 h and kept in a desiccator at room temperature.

### Batch biosorption

For batch sorption experiments, 50.0 mg of A.C. was introduced into an Erlenmeyer flask containing 50 mL solution with 50 mg L<sup>-1</sup> lead (II) ions. The pH of solution was adjusted by adding a small amount of diluted HNO<sub>3</sub> or NaOH to the original lead (II) solution, and then, the pH was measured using a pH meter (Martini Instruments, Mi 150,

Romania). The aforementioned glass flasks were transferred to an incubator shaker (FaraAzma 911,201, Iran) under a constant shaking speed of 150 rpm for 2 h at 25 °C and then the sorbent was filtered. The lead ion species distribution was calculated using Visual Minteq software with the initial Pb (II) concentration of 50 mgL<sup>-1</sup>.

The competing experiments were performed by adding Na<sup>+</sup>, Mg<sup>2+</sup> and Ca<sup>2+</sup> ions at different concentrations to the initial 50 mgL<sup>-1</sup> Pb (II) at 25 °C, with 50.0 mg sorbent at pH = 5.8 ± . The contents of each flask were transferred to an incubator shaker for 2 h of shaking to reach sorption equilibrium. Finally, the residual lead concentrations were calculated using the flame atomic absorption spectrophotometer (FAAS).

### Isotherms and thermodynamics of A.C. biosorption

In order to confirm the sorption mechanism, the rate of Pb (II) sorption process on A.C. was performed. For this purpose, 0.5 g of A.C. was added into a 500 mL solution containing 50 mg L<sup>-1</sup> of lead ions. Mechanical stirring was used to attain full mixing, and 0.5 mL of the solution was sampled at a specific time. The sample concentrations and sampling time were reported to calculate sorption rates.

Sorption isotherms were determined to evaluate the maximum sorption capacity. Briefly, 50.0 mg of treated A.C. was introduced into series flasks containing 50 mL of solution with different concentrations of lead (II) ions (40, 60, 80, 100, 150, 200 and 300 mg L<sup>-1</sup>) while the pH of the solution at equilibrium was adjusted to 5.8 ± 0.2. These flasks were transferred to an incubator shaker for 2 h of shaking. Subsequently, the lead ions were determined and the maximum sorption capacity calculated by the classic Langmuir or Freundlich models. Finally, thermodynamic parameters were calculated at various temperatures.

### Equilibrium experiments and data evaluation

For all batch biosorption experiments, the removal efficiency (E) and adsorption capacity  $q_e$  (mg g<sup>-1</sup>) of Pb (II) on A.C. at equilibrium in the aqueous solution were calculated according to the following equation:

$$E = \frac{(C_0 - C_e)}{C_0} \times 100 \quad (1)$$

$$q_e = \frac{(C_0 - C_e)V}{W} \quad (2)$$

where  $C_0$  (mg L<sup>-1</sup>) and  $C_e$  (mg L<sup>-1</sup>) represent the initial and equilibrium concentrations of lead ions, respectively;  $V$  (L) is the volume (lead ions solution); and  $W$  (g) is the mass of A.C. In the current study, the effect of some essential



parameters such as initial pH, shaking time and concentration of Pb ions was optimized. All experiments were performed in triplicates.

## Results and discussion

### Characterization of the Artemia cyst

Before and after biosorption, A.C. were characterized by FT-IR analysis, SEM, EDS and XRD. FT-IR pattern of the samples before and after lead ions adsorption was recorded to identify the possible functional groups of A.C. (Fig. 1). The broad peak at  $\sim 3377\text{ cm}^{-1}$  was assigned to hydrogen-bonding of O–H and –N–H (Zhang et al. 2017). The weaker peaks at  $\sim 2958$  and  $2927\text{ cm}^{-1}$  were assigned to the C–H<sub>n</sub> stretching groups (Yang 2007). The peaks at  $1399\text{ cm}^{-1}$  and  $\sim 1451\text{ cm}^{-1}$  were corresponding to the C–OH stretching and bending vibration group, respectively (Fan et al. 2013). A sharp peak appearing in the region  $1653\text{ cm}^{-1}$  can be attributed to the C=O stretch bending (Gupta and Rastogi 2008). The peak at  $\sim 1240\text{ cm}^{-1}$  and the strong peak at  $\sim 1542\text{ cm}^{-1}$  may indicate the presence of amide I (C–N, N–H) and amide II groups, respectively (Van De Velde and Kiekens 2004; Wang et al. 2018). In summary, these results represent the chitin and amino acids components on shell structure.

In this sample, shifting of the OH vibration band to an upper value and increasing in its intensity were observed which is due to the OH groups that bonded with lead ions. In addition, peaks at  $2927$ ,  $2851$  and  $1542\text{ cm}^{-1}$  were observed to have shifted to  $2925$ ,  $2855$  and  $1537\text{ cm}^{-1}$ , respectively. On the other hand, the large band had shifted 5 wavenumbers for amide II component ( $1537\text{ cm}^{-1}$ ) and the peak intensity increased. These significant shifts might be attributed to the

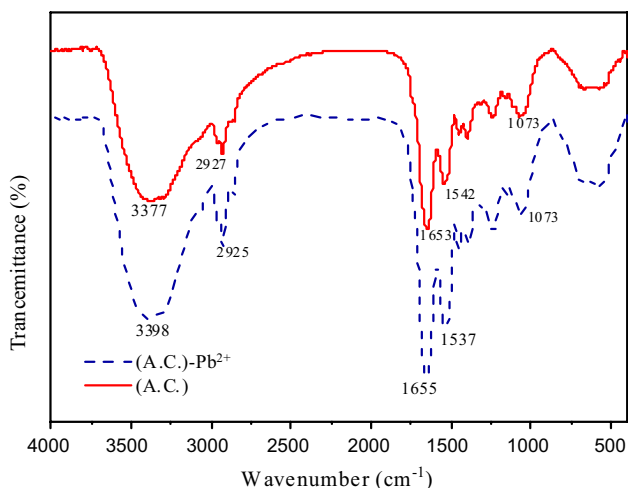


Fig. 1 FT-IR spectra of the A.C. after and before Pb ions uptake

formation of a strong bond between the –NH group and lead ion.

SEM images of A.C. are presented in Fig. 2a–f. As demonstrated in Fig. 2a, the size of spherical cysts is about 150–250  $\mu\text{m}$ . Remarkably, Fig. 2b, 2c show the chorion layer and outer cuticular membrane of cyst with 3D hierarchical morphology structure while size ranges of pores are widespread. The pore size distribution of A.C. shows the wide distribution from 100 to 1000 nm.

The macro-pore size and pore volume of sorbent was adopted to capturing heavy metal ions from contaminated water (Awual 2015; Kubra et al. 2021).

Figure 2d, e is shown the A.C. after uptake of lead ions. After biosorption process, the pores have been covered and they are not visible as presented in Fig. 2f). These changes demonstrate the capturing of lead ions by several functional groups (carboxyl and amides) that have been expanded on the surface of cysts. Concurrently, the EDS results before and after the lead ions uptake confirm these observations (Fig. 3a, b). The sharp peak corresponds to lead ions and it affirms the high uptake of these ions on Artemia cyst surface. Furthermore, it indicates that the essential elements such as C, O, P and K integrate with chitin components and amino acids in cyst shell.

XRD pattern of A.C. before and after lead (II) uptake is shown in Fig. 3c. The noisy pattern and broad peak of cysts suggest an amorphous structure or an alternative conclusion that can be drawn is that the degree of crystallinity is low. The characteristic peaks at  $2\theta$  values of 8.66 and 20.26 are, respectively, corresponding to (0 2 0) and (1 1 0) diffraction planes of cyst chitin (Zhou et al. 2005a; Liu et al. 2020). After lead uptake, the new distinct peaks at  $2\theta$  values of 25.76 and 30.21 are observed adsorption of lead ions in samples (Zhou et al. 2005b). The characterization result suggests the high affinity Pb ions. Next, the affecting biosorption parameters were further elucidated.

### Optimization of experimental parameters

#### Effects of pH on Pb(II) uptake

According to the previous studies, the biosorption process is highly pH dependent that influences on metal chemistry and binding functional groups (Awual et al. 2020b). Hence, in this research, the effect of pH (ranging from 2.0 to 7.0 chosen based on the alpha distribution functions of lean ions species shown in Fig. 4b) on lead ions uptake was investigated to provide an extensive insight on the sorption process. As apparent in Fig. 4a adsorption procedure of lead ions onto A.C. is divided to several stages. For  $\text{pH} < 2.5$  (low adsorption phase), uptake efficiency of lead ions diminishes as a consequence of protonating of functional groups such as amides/carboxyl component on the surface of cysts



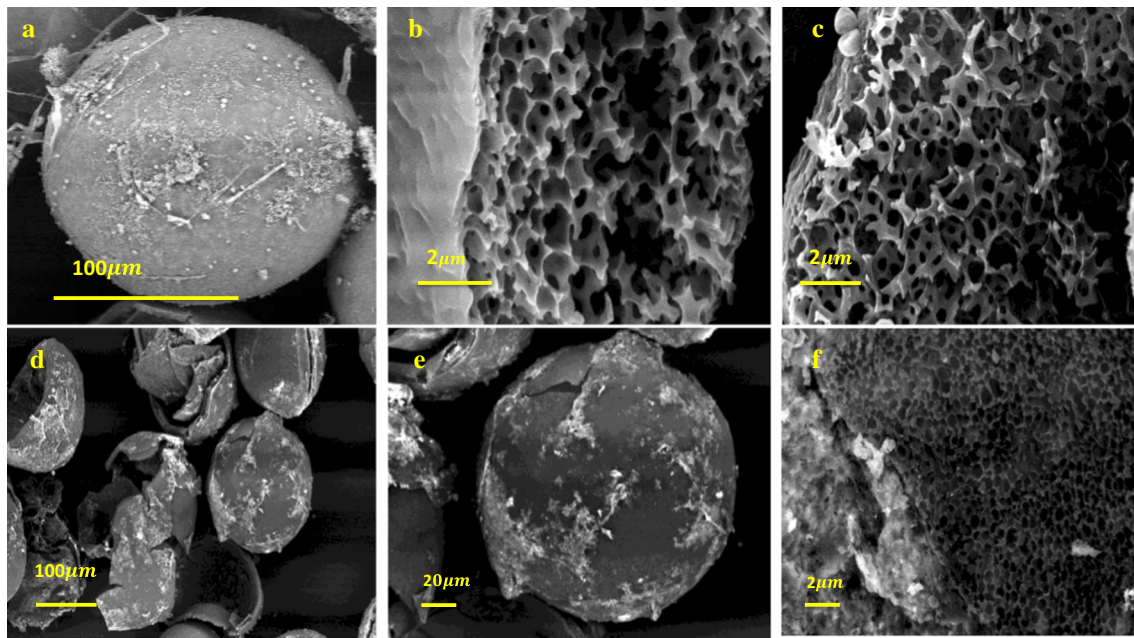


**Fig. 2** SEM images before uptake of lead ions for (a) cyst of *Artemia*; (b) chorion layer and outer cuticular membrane of cyst; (c) pore structures of the inner porous of cysts; and SEM images after uptake lead ions for (d, e) cyst of *Artemia*; (f) pore structure of the inner porous of cysts

which lead to deactivation of metal adsorption sites. The sharp stage (pH = 3 – 5.5) was exhibited by increasing pH and slope of the graph enhances to reach the maximum sorption capacity stage. In the next stage (pH = 5.5–6), graph slope is almost constant which is due to saturation of all the sorption sites during previous stages. Accordingly, pH = 5.8 was considered as the optimum condition pH value in all the experiments to avoid any hydroxide precipitation.

Moreover, lead hydroxide,  $\text{Pb}(\text{OH})_2$ , precipitated in the high pH levels (pH  $\geq$  7). Nature of lead ion, aqua solution condition and nature of cysts are essential factors which affect biosorption of lead ions.

The distribution of lead ion species is demonstrated in Fig. 4b based on the alpha distribution functions and step-wise formations constants of each species. As shown in this figure, the dominant form of lead ions at selective pH range was mainly  $\text{Pb}(\text{II})$  with a trace level of  $\text{Pb}(\text{OH})^+$  but more than 90% biosorption of  $\text{Pb}(\text{II})$  occurred and precipitation was not observed at optimum pH. It is possible that due to the presence of trace amounts of other lead ion species such as  $\text{Pb}(\text{OH})^+$  which is distinct from  $\text{Pb}(\text{II})$  ion in the complex formation constant,  $\text{Pb}(\text{II})$  uptake is slightly reduced. More significantly, at pH < 2 unsaturation of sorbent occurred in acidic solution.

### Biosorption selectivity

Selectivity is argued as one of the essential parameters for successful adsorbent process. Most of the materials that have

large capacities for ions adsorption do not accomplish effective performance owing to powerful competing affinity of different ions for the same adsorbent, i.e., A.C. As established in earlier studies, the general cations including  $\text{Na}^+$ ,  $\text{Ca}^{2+}$  and  $\text{Mg}^{2+}$  at high concentrations are present in natural aqua environment of *Artemia* cysts.

Thus, they influence lead biosorption selectivity. In this study, to assess the effective possible competing ions on biosorption efficiency, the competing cations were examined in the presence of lead ions at optimum experiment condition (pH: 5.8,  $0.5 \text{ g L}^{-1}$  sorbent at  $25^\circ\text{C}$ ) and the results are given in Fig. 5a–c. As the results suggest, lead ions uptake decreased in the presence of  $\text{Mg}^{2+}$  and  $\text{Ca}^{2+}$  particularly when the  $\text{Ca}^{2+}$  was applied while A.C. still acted as a favorable sorbent for  $\text{Pb}(\text{II})$  even at 100 times comparative cations addition.

Functional groups are playing an essential key for ion selectivity study (Awual 2019a; Awual et al. 2020a). This selective behavior of cysts could be ascribed by the existence of high number of functional groups such as amides and carboxyl on the surface and 3D structure of cyst with various pore sizes that are not easily saturated. Whereas, in the presence of  $\text{Na}^+$ , after a little decrease,  $\text{Pb}$  ions uptake increased over the initial  $\text{Pb}$  uptake without interference. It has been suggested that biosorption is naturally non-electrostatic (Liu et al. 2013). Furthermore, the presence of salt ions may decrease the negative charge density of the double layer, and therefore, higher the lead ion biosorption (Liu et al. 2013). Additionally, selectivity coefficient has been



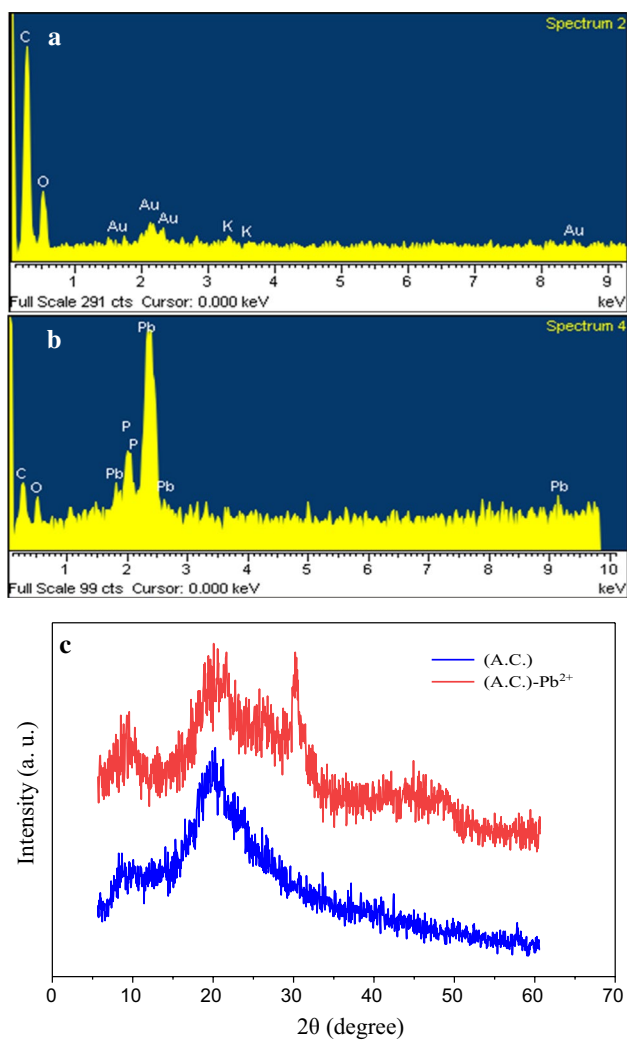


**Fig. 3** EDS spectra of cyst of Artemia (a) before and (b) after Pb ions uptake; (c) X-ray diffraction patterns (XRD) of (A.C.) after and before Pb ions uptake

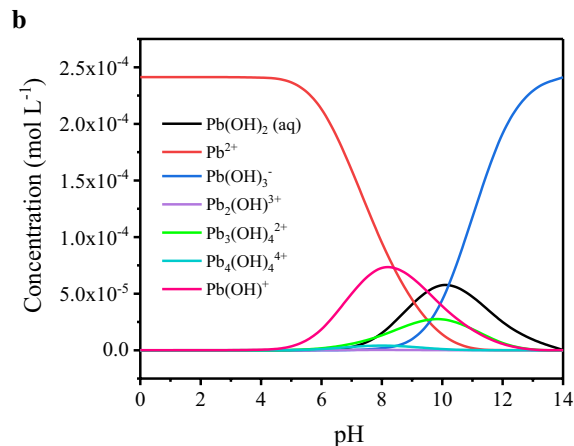
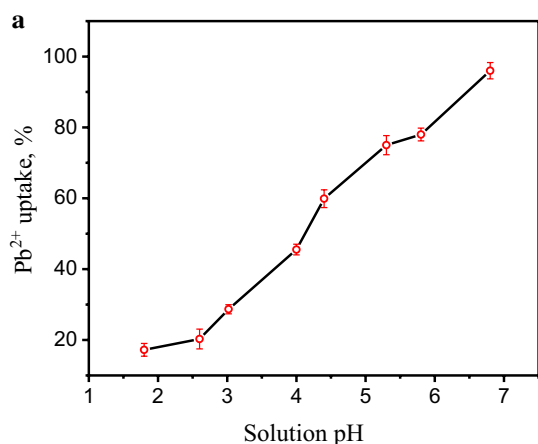


**Fig. 4** (a) pH effects on Pb(II) uptake (conditions: 0.5 g L<sup>-1</sup> sorbent, initial lead (II) concentration of 50 mg L<sup>-1</sup> at 25 °C); (b) Pb<sup>2+</sup> species distribution at different pH values of solution

investigated using microalgae in aqueous solution and the results suggest that:  $\text{Na}^+ < \text{H}^+ < \text{Cd}^{2+} < \text{Pb}^{2+}$ . The higher affinity for lead ions might be justified based on the hard and soft acid–base theory (Hackbarth et al. 2013). This signifies a key result since the cysts of Artemia hatch in high concentration of salt and makes the application of this method operational.

The selectivity distribution ratio,  $K_d$  (mLg<sup>-1</sup>), was defined to quantify the biosorption selectivity with Eq. 3 (Wan et al. 2016) and the results are shown in Table 1.

$$K_d = \frac{(C_0 - C_e)}{C_e} \times \frac{V}{M} \quad (3)$$

As disclosed in Table 1, the large  $K_d$  values for A.C. samples verify their excellent selectivity and preferential biosorption performances.

Also, several divers metal ions presented in wastewater samples that influence heavy metal ions uptake. Therefore, interfering mixed metal ions such as  $\text{Cd}^{2+}$ ,  $\text{Mn}^{2+}$ ,  $\text{Co}^{2+}$ ,  $\text{Cu}^{2+}$ ,  $\text{Ca}^{2+}$ ,  $\text{Ni}^{2+}$  and  $\text{Mg}^{2+}$  on lead ion biosorption by A.C. were investigated and the results are depicted in Fig. 5d. The data demonstrated the presence of mixed metal ions with a faintly lower biosorption when compared to single ion biosorption. The biosorption percentage was 73.5%. In this experiment, the foreign metal ion concentrations were 20-fold higher than that of the  $\text{Pb}^{2+}$  concentration in the sample solution.

#### Effect of initial lead ions concentration

To determine the role of initial lead (II) ions concentration on the uptake efficacy, diverse concentrations of lead ions ranging from 20 to 300 mgL<sup>-1</sup> were studied (Fig. 5e). As demonstrated, the Pb(II) uptake increased and then



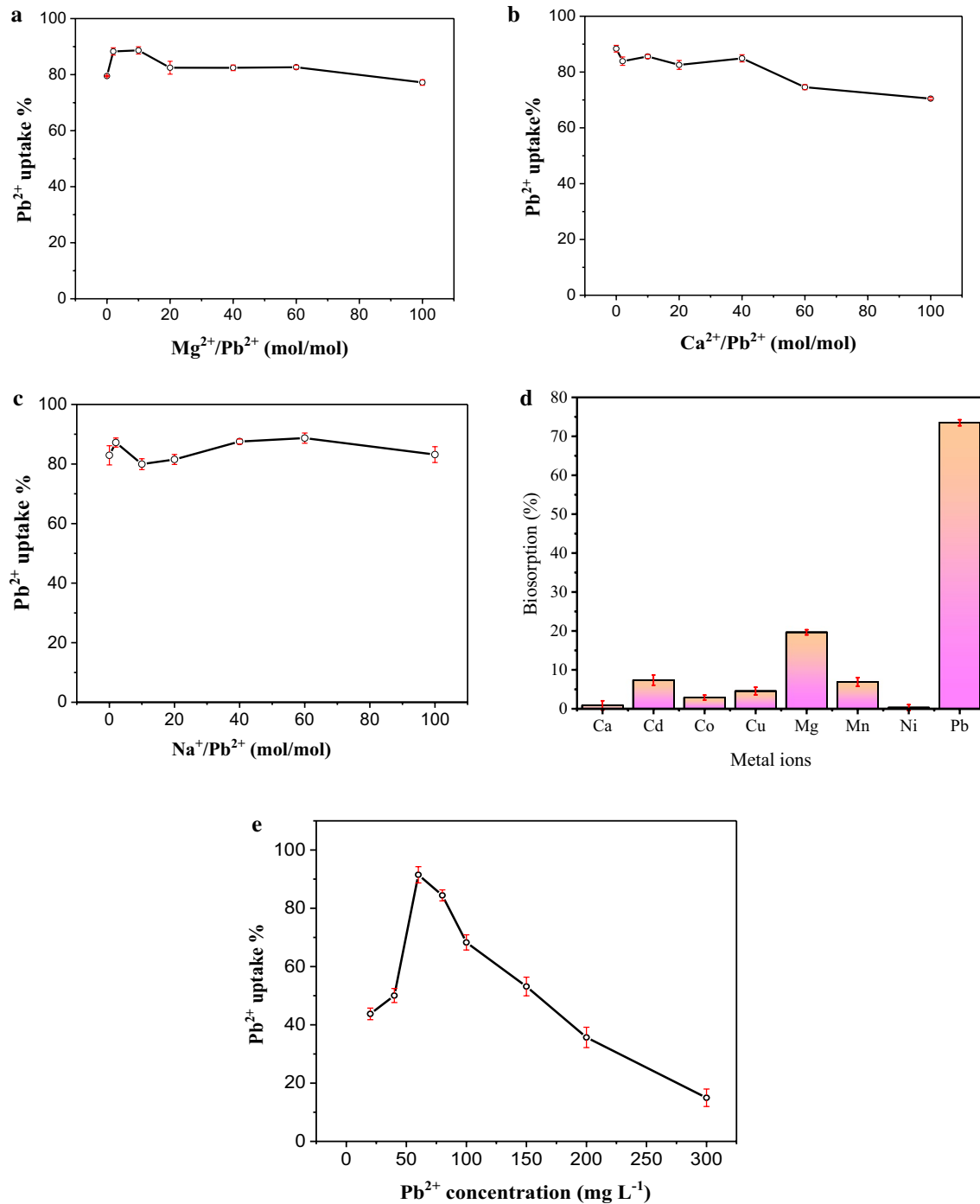


**Fig. 5** Biosorption selectivity evaluation (a–c) for the effects of Mg, Ca and Na ions on lead ions uptake by A.C., respectively. (Pb(II) concentration 50 mg L<sup>-1</sup>) (d) competing cations effect for Pb (II) biosorption (Pb(II) concentration 1 mg L<sup>-1</sup>, competing ion concen-

tration was 20.0 mg L<sup>-1</sup>) and (e) effect of initial Pb ions concentration on uptake by A.C. ( optimum conditions: 0.5 g L<sup>-1</sup> sorbent, pH=5.8±0.2, T=25 °C, volume=50 mL.)

gradually decreased. Maximum Pb (II) uptake of the A.C. was observed to be 92% when the initial lead concentration was 60 mgL<sup>-1</sup>. Furthermore, after 60 mgL<sup>-1</sup> initial concentration of lead ions, lead uptake percentage decreases which may be due to saturation of adsorption sites on the

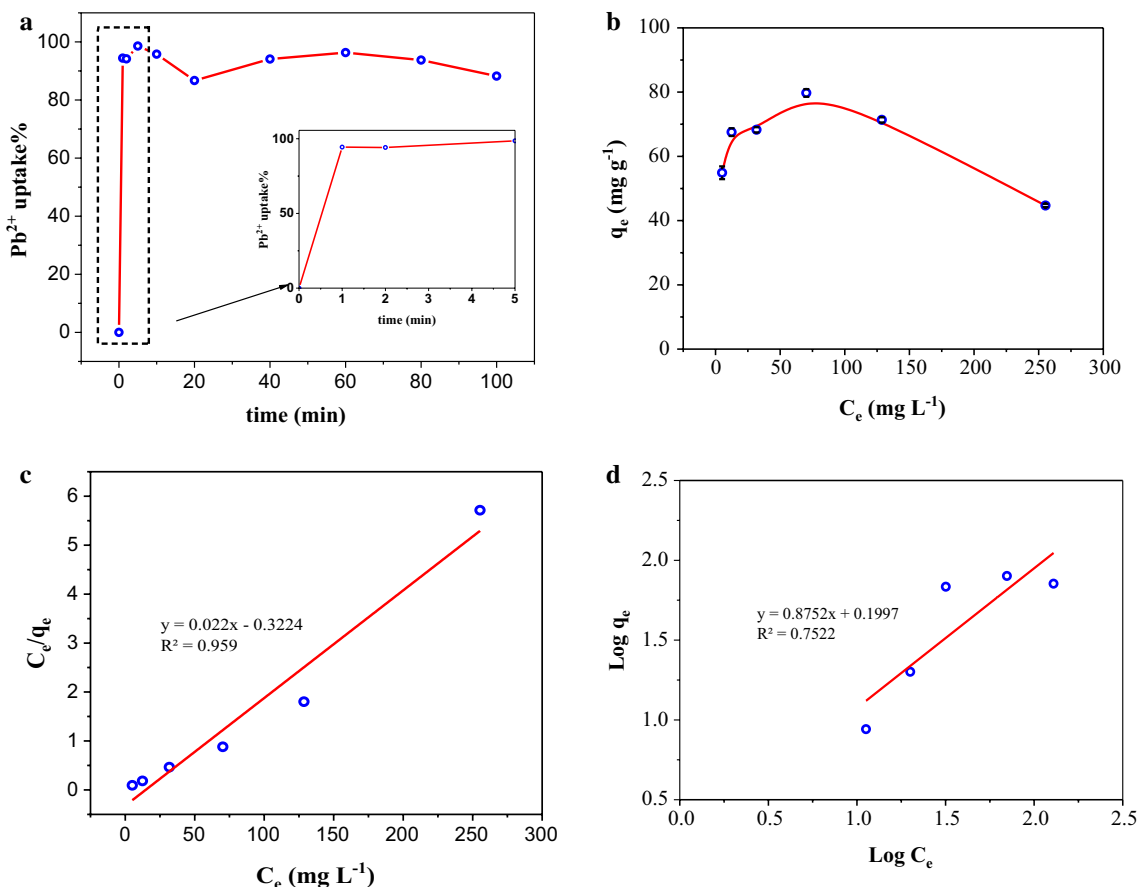
A.C. In order to test the effect of lead toxicity on A.C. hatching, cysts were exposed to 60 mg L<sup>-1</sup> of lead ions under hatching condition. Interestingly, it was observed that nauplii were hatched in this condition. Additional data are given in Online Resource (ESM\_1.mp<sub>4</sub>). This experiment confirms





**Table 1**  $K_d$  ( $\text{mL g}^{-1}$ ) Values of lead ions biosorption onto A.C. in the presence of competing ions at different levels

Competing ions (M)	$K_d$ ( $\text{mL g}^{-1}$ ) at different ratios of M/Pb(II)					
	2	10	20	40	60	100
$\text{Na}^+$	6825.95	3990.02	4417.71	7034.71	7855.83	4941.07
$\text{Ca}^{2+}$	5209.64	5936.74	4735.92	5632.18	2933.91	2387.53
$\text{Mg}^{2+}$	7528.06	7813.68	4699.31	4690.87	4762.36	3382.12

**Fig. 6** (a) Biosorption rate at different time intervals (conditions:  $0.5 \text{ g L}^{-1}$  sorbent, initial lead(II) concentration of  $50 \text{ mg L}^{-1}$  at  $25 \text{ }^\circ\text{C}$ , volume:  $500 \text{ mL}$ ,  $\text{pH} = 5.8 \pm 0.2$ ). (b) Biosorption isotherm, (c) Lang-muir isotherm and (d) Freundlich isotherm (condition:  $0.5 \text{ g L}^{-1}$  sorbent,  $25 \text{ }^\circ\text{C}$ ,  $\text{pH} = 5.8 \pm 0.2$ )

our conclusion that hatching might be safe under contaminated environment.

Additionally, sensitivity was calculated by series of lead ion concentrations which were used for plotting curve. Correlation coefficients ( $R^2$ ) and sensitivity were obtained 0.9979 and 0.0105, respectively, for  $y = 0.018x + 0.007$ .

### Lead ions rate and isotherms

Biosorption rate was conducted to determine the biosorption process (Fig. 6a). An acutely rapid lead ion uptake was found in less than one minute with approximately 95% uptake efficiency which lasted until the end of 100 min. This

extreme biosorption can be credited to the pore morphology and functional groups in cysts. Similarly, in a recent work, ion uptake by cyst shells occurred in approximately 2 min (Wang et al. 2018). However, more time was used in all experiments to ensure lead ion biosorption.

The macroscale pores can execute fast lead ions adsorption while the meso-/micro-pore scale can support more surface area and active sites for biosorption. Some studies show adsorption rate that is regarded as one of the disadvantages for the process (Meena et al. 2005; Soares et al. 2016). For instance, in a study by Hua, M. et al. the adsorption process improved through nanocomposite fabrication results in modification of the porous polystyrene (Hua et al. 2013).



As illustrated in the results, A.C. represent high capacity for lead uptake. In this study, A.C. can uptake Pb ions through functional groups especially amine and this process is distinct.

The adsorption isotherm is a pivotal parameter in designing the adsorption process and evaluation of the adsorbent performance. Two major adsorption isotherm models applied mostly in water treatment are Freundlich and Langmuir. Langmuir isotherm is the most widely used in adsorption studies. Monolayer coverage on the biosorbent, constant adsorption energy, homogeneous adsorption sites and no interaction between the adsorbed molecules or ions are major assumptions of Langmuir isotherm. This model is expressed in Eq. (4) (Li et al. 2011; Guo and Wang 2019).

$$\frac{C_e}{q_e} = \frac{1}{q_m K_l} + \frac{C_e}{q_m} \quad (4)$$

where  $C_e$  is the equilibrium concentration of lead ions in solution ( $\text{mgL}^{-1}$ ),  $q_e$  is the adsorbed value of lead ions at equilibrium concentration ( $\text{mg g}^{-1}$ ),  $q_m$  is the maximum adsorption capacity on adsorbent ( $\text{mg g}^{-1}$ ), and  $K_l$  is the Langmuir constant that is related to the adsorption energy ( $\text{L mg}^{-1}$ ) (Malik et al. 2018).

Another parameter that can be defined using the Langmuir equation is the separation factor, which is represented by  $R_l$  and is defined according to the following Eq. (5):

$$R_l = \frac{1}{1 + K_l C_0} \quad (5)$$

where  $K_l(\text{Lmg}^{-1})$  and  $C_0(\text{mgL}^{-1})$  are Langmuir isotherm constant and initial lead ions concentration, respectively.

The values of  $R_l$  indicate the type of equilibrium reaction for the adsorption process. If the value of  $R_l$  is zero, the adsorption is the non-equilibrium reaction type, and if it is ( $0 < R_l < 1$ ), ( $R_l = 1$ ) or ( $R_l > 1$ ), the adsorption type is optimal, linear and undesirable, respectively. Therefore, the Langmuir isotherm can explain the maximum capacities and the surface properties of the adsorbent (Wang and Guo 2020). The Freundlich isotherm is considered to model multilayer adsorption and heterogeneous process on adsorbent. It can be described as Eq. 6:

$$\text{Log} q_e = \text{Log} k_f + \frac{1}{n} \text{Log} C_e \quad (6)$$

where  $k_f$  ( $\text{mg g}^{-1}$ ) and  $n$  are the Freundlich constants, indicating the biosorption capacity and the biosorption intensity in the solution, respectively.

The isotherm study of lead ion biosorption was performed and is shown in Fig. 6b. The data were further fitted to Langmuir and Freundlich models to select the best model. Maximum lead ion capacity was observed  $79.75 \text{ mg g}^{-1}$ .

**Table 2** Constants and parameters of adsorption isotherms for the lead adsorption

Model	Parameter	R <sup>2</sup>
Freundlich	$K_f$ ( $\text{mg g}^{-1}$ ) = 1.583 $n = 1.142596$	0.7522
Langmuir	$q_m$ ( $\text{mg g}^{-1}$ ) = 45.45 $K_l(\text{Lmg}^{-1}) = 0.068$	0.959

Figure 6c, d exhibits the maximum lead ion uptake capacity by applying Langmuir and Freundlich models. The detailed equation and constant values are given in Table 2. The data shown in Table 2 fitted well in Langmuir adsorption isotherm.

It indicates that the biosorption has occurred at homogeneous sites in surface of cysts and the rate limiting step is diffusion. In addition, a value of  $R_l$  between 0 and 1 for all concentrations at  $25^\circ\text{C}$  specifies the favorable adsorption (Table 3).

### Effect of temperature on biosorption

Thermodynamic parameters of the biosorption process such as Gibbs free energy ( $\Delta G^\circ$ ), enthalpy ( $\Delta H^\circ$ ) and entropy ( $\Delta S^\circ$ ) have been calculated to determine the effect of temperature on lead ions uptake at 298, 313 and 333 K. These parameters can be calculated by the following equation:

$$\Delta G^\circ = -RT \ln (K_e) \quad (7)$$

$$\ln K_e = \left( \frac{\Delta S^\circ}{R} \right) - \left( \frac{\Delta H^\circ}{RT} \right) \quad (8)$$

$$K_e = \frac{q_e}{C_e} \quad (9)$$

where  $K_e$  is the biosorption equilibrium constant ( $\text{mL g}^{-1}$ ),  $R$  is the universal gas constant ( $8.314 \text{ J mol}^{-1} \text{ K}^{-1}$ ), and  $T$  is the absolute temperature (K). The Gibbs free energy change values for the biosorption of lead ions are negative, indicating that the biosorption process by A.C. is feasible and spontaneous. The low values of  $\Delta G^\circ$  with increase in temperature indicate not efficient biosorption at higher temperature.

Furthermore, the Van't Hoff equation shown in Eq. 7, enthalpy ( $\Delta H^\circ$ ) and entropy ( $\Delta S^\circ$ ) were calculated from the plot of  $\ln K_d$  versus  $1/T$ . The thermodynamic parameters are recorded in Table 4. As revealed in this table, the enthalpy and entropy values were negative. The negative value of enthalpy indicates that the biosorption is exothermic in nature and the negative value of entropy corroborates the decreased randomness at the cyst egg-solution interface during the lead ion uptake. The maximum



**Table 3**  $R_1$  values by A.C. for the lead adsorption at different initial concentrations

$C_0$ ( $\text{mg L}^{-1}$ )	20	40	60	80	100	150	200	300
$R_1$	0.423	0.268	0.196	0.155	0.128	0.089	0.068	0.046

**Table 4** Thermodynamic parameters for the biosorption of lead ions on A.C

T (K)	$\Delta G^\circ$ ( $\text{kJ mol}^{-1}$ )	$\Delta H^\circ$ ( $\text{kJ mol}^{-1}$ )	$\Delta S^\circ$ ( $\text{J mol}^{-1} \text{K}^{-1}$ )
298	-3.24	-28.74	-86.133
313	-1.46		
333	-0.22		

uptake of lead ions was observed at 298 K. Thus, the biosorption of lead ions on the cyst of Artemia decreased by increasing the temperature due to the exothermic process.

Various sorbents for lead ions uptake reported in literature are summarized in Table 5. This table shows fast lead ion uptake by A.C. In addition to natural biosorbents, there are many studies reported in the literature regarding the toxic diverse metal ions removal based on the composite ensemble materials. The advantages including high selectivity and sensitively, efficiency of lead ion adsorption from aqueous solution and other parameters are summarized in Table 5. Chemical composites require efforts to synthesize and impose high cost to metal ion removals despite the fact the efficiency of removal is some cases might higher than biosorbents (Awual 2019b; Awual et al. 2019, 2020a).

**Table 5** Comparison of lead ion adsorption/ biosorption with various materials

Sorbent	$q_m$ ( $\text{mg g}^{-1}$ )	Time (min)	pH	Selectivity	Method	References
Conjugate material (CM)	196.35	50	6	S <sup>c</sup>	AS <sup>a</sup>	Awual (2019b)
Mesoporous silica and conjugate material (MCM)	179.82	60	5.20	S	AS	Awual et al. (2019)
Mesoporous silica monolith	176.66	50	5.50	S	AS	Awual et al. (2020a)
Eggshell-rich composite	23.3	180	5	NR <sup>d</sup>	BS <sup>b</sup>	Soares et al. (2016)
Cucumber peel	133.60	60	5	NR	BS	Basu et al. (2017)
Saffron flower waste	45.6	9	6	NR	BS	Khoshsang and Ghaffarinejad (2018)
Artemia cyst	79.75	1	5.8	S	BS	This study

<sup>a</sup>Adsorption<sup>b</sup>Biosorption<sup>c</sup>Selective<sup>d</sup>Not reported

## Conclusion

In summary, we propose to apply Artemia cyst as a robust lead ions biosorbent that provides rapid and effectual Pb ions uptake. Special 3D morphology pore structure and functional groups in surface of Artemia cysts can make them preeminent biosorbents. Artemia cysts surface was characterized by FT-IR, SEM, EDS and XRD and the results showed successful lead ions uptake. Batch biosorption occurred in one minute with 94.40% uptake efficiency. The maximum biosorption capacity was  $79.75 \text{ mg g}^{-1}$  at the optimum pH = 5.8 at 25 °C with  $0.5 \text{ g L}^{-1}$  sorbent. Moreover, Artemia cysts revealed impressive selectivity and applicability in the presence of common available ions in their natural environment ( $\text{Ca}^{2+}$ ,  $\text{Mg}^{2+}$  and  $\text{Na}^+$ ) at elevated levels. The ICP result also showed 73.5% lead ion uptake in common heavy metal ions in wastewater. Finally, the biosorption data best fitted with the Langmuir isotherm and thermodynamic parameter showed this processes exothermic and spontaneous.

Results of this study consequentially lead to the recommendation new concept of using Artemia cyst with astounding uptake of lead ions as a green approach comprising of a biocompatible sorbent that evades the utilization of any chemical components that inevitably cause irreversible damage to the natural ecosystem. More importantly, given that A.C. are living organisms, which are characterized as adsorbents of high endurance in addition to their cost-effectiveness in comparison with the existing methods. The authors

of this research hope to have opened a gate toward continuity of sorption systems of contaminants in aqueous solutions and little by little envision a healthier environment for the livelihood and survival of these organisms. Further studies need to be carried out in order to shorten the adsorption time and increasing the efficiency as well as the selectivity of the process.

**Supplementary Information** The online version contains supplementary material available at <https://doi.org/10.1007/s13762-021-03844-8>.

**Acknowledgements** As authors of the article, we acknowledge Ferdowsi University of Mashhad for supporting this project (Grant Number: 3/51645)

**Author contribution** Somayyeh Ziaei: data collection, sample analysis, writing—original draft and data interpretation. Hossein Ahmadzadeh: conceptualization, data analysis, funding acquisition, project supervision and data validation. Zarrin Es'baghi: conceptualization, data analysis, writing—review & editing.

**Funding** This study is funded by Ferdowsi University of Mashhad (Grant Number: 3/51645).

## Declarations

**Conflicts of Interest** The authors declare no conflicts of interest.

## References

- Awual MR (2015) A novel facial composite adsorbent for enhanced copper(II) detection and removal from wastewater. *Chem Eng J* 266:368–375. <https://doi.org/10.1016/j.cej.2014.12.094>
- Awual MR (2019a) Innovative composite material for efficient and highly selective Pb(II) ion capturing from wastewater. *J Mol Liq* 284:502–510. <https://doi.org/10.1016/j.molliq.2019.03.157>
- Awual MR (2019b) Mesoporous composite material for efficient lead(II) detection and removal from aqueous media. *J Environ Chem Eng* 7:103124. <https://doi.org/10.1016/j.jece.2019.103124>
- Awual MR, Hasan MM (2019) A ligand based innovative composite material for selective lead(II) capturing from wastewater. *J Mol Liq* 294:111679. <https://doi.org/10.1016/j.molliq.2019.111679>
- Awual MR, Hasan MM, Iqbal J et al (2020a) Naked-eye lead(II) capturing from contaminated water using innovative large-pore facial composite materials. *Microchem J* 154:104585. <https://doi.org/10.1016/j.microc.2019.104585>
- Awual MR, Hasan MM, Islam A et al (2019) Offering an innovative composited material for effective lead(II) monitoring and removal from polluted water. *J Clean Prod* 231:214–223. <https://doi.org/10.1016/j.jclepro.2019.05.125>
- Awual MR, Yaita T, Kobayashi T et al (2020b) Improving cesium removal to clean-up the contaminated water using modified conjugate material. *J Environ Chem Eng* 8:103684. <https://doi.org/10.1016/j.jece.2020.103684>
- Basu M, Guha AK, Ray L (2017) Adsorption of Lead on Cucumber Peel. *J Clean Prod* 151:603–615. <https://doi.org/10.1016/j.jclepro.2017.03.028>
- Bergami E, Bocci E, Vannuccini ML et al (2016) Nano-sized polystyrene affects feeding, behavior and physiology of brine shrimp *Artemia franciscana* larvae. *Ecotoxicol Environ Saf* 123:18–25. <https://doi.org/10.1016/j.ecoenv.2015.09.021>
- Bolisetty S, Peydayesh M, Mezzenga R (2019) Sustainable technologies for water purification from heavy metals: review and analysis. *Chem Soc Rev* 48:463–487. <https://doi.org/10.1039/C8CS00493E>
- Bowman N, Patel D, Sanchez A et al (2018) Lead-resistant bacteria from Saint Clair River sediments and Pb removal in aqueous solutions. *Appl Microbiol Biotechnol* 102:2391–2398. <https://doi.org/10.1007/s00253-018-8772-4>
- Brown E (2012) *World Fish Farming: Cultivation and Economics*. Springer, US
- Cashin VB, Eldridge DS, Kingshott P, Yu A (2018) Distinguishing surface sites involved in the adsorption of lead onto sinapinaldehyde-functionalised mesocellular foam mesoporous silica. *Colloids Surfaces A Physicochem Eng Asp* 552:153–160. <https://doi.org/10.1016/j.colsurfa.2018.05.021>
- Chatterjee S, Mondal S, De S (2018) Design and scaling up of fixed bed adsorption columns for lead removal by treated laterite. *J Clean Prod* 177:760–774. <https://doi.org/10.1016/j.jclepro.2017.12.249>
- Chen W, Lu Z, Xiao B et al (2019) Enhanced removal of lead ions from aqueous solution by iron oxide nanomaterials with cobalt and nickel doping. *J Clean Prod* 211:1250–1258. <https://doi.org/10.1016/j.jclepro.2018.11.254>
- Clegg JS, Jackson SA, Warner AH (1994) Extensive Intracellular Translocations of a Major Protein Accompany Anoxia in Embryos of *Artemia franciscana*. *Exp Cell Res* 212:77–83. <https://doi.org/10.1006/excr.1994.1120>
- Fan L, Luo C, Sun M et al (2013) Colloids and Surfaces B: Biointerfaces Highly selective adsorption of lead ions by water-dispersible magnetic chitosan / graphene oxide composites. *Colloids Surfaces B Biointerfaces* 103:523–529. <https://doi.org/10.1016/j.colsurfb.2012.11.006>
- Guo X, Wang J (2019) Comparison of linearization methods for modeling the Langmuir adsorption isotherm. *J Mol Liq* 296:111850. <https://doi.org/10.1016/j.molliq.2019.111850>
- Gupta VK, Rastogi A (2008) Biosorption of Lead from Aqueous Solutions by Green Algae *Spirogyra* Species: Kinetics and Equilibrium Studies 152:407–414. <https://doi.org/10.1016/j.jhazmat.2007.07.028>
- Hackbarth FV, Girardi F, de Souza SMAGU et al (2013) Marine macroalgae *Pelvetia canaliculata* (Phaeophyceae) as a natural cation exchanger for cadmium and lead ions separation in aqueous solutions. *Chem Eng J* 242:294–305. <https://doi.org/10.1016/j.cej.2013.12.043>
- Hannachi Y, Hafidh A (2020) Biosorption potential of *Sargassum muticum* algal biomass for methylene blue and lead removal from aqueous medium. *Int J Environ Sci Technol* 17:3875–3890. <https://doi.org/10.1007/s13762-020-02742-9>
- Hossain MA, Ngo HH, Guo WS et al (2014) Competitive adsorption of metals on cabbage waste from multi-metal solutions. *Bioresour Technol* 160:79–88. <https://doi.org/10.1016/j.biortech.2013.12.107>
- Hua M, Jiang Y, Wu B et al (2013) Fabrication of a New Hydrous Zr(IV) Oxide-Based Nanocomposite for Enhanced Pb(II) and Cd(II) Removal from Waters. *ACS Appl Mater Interfaces* 5:12135–12142. <https://doi.org/10.1021/am404031q>
- Huang Z-H, Zheng X, Lv W et al (2011) Adsorption of Lead(II) Ions from Aqueous Solution on Low-Temperature Exfoliated Graphene Nanosheets. *Langmuir* 27:7558–7562. <https://doi.org/10.1021/la200606r>
- Khoshsang H, Ghaffarinejad A (2018) Rapid removal of lead (II) ions from aqueous solutions by saffron flower waste as a green biosorbent. *J Environ Chem Eng* 6:6021–6027. <https://doi.org/10.1016/j.jece.2018.09.020>
- Koley P, Sakurai M, Aono M (2016a) Controlled Fabrication of Silk Protein Sericin Mediated Hierarchical Hybrid Flowers and Their



- Excellent Adsorption Capability of Heavy Metal Ions of Pb(II), Cd(II) and Hg(II). *ACS Appl Mater Interfaces* 8:2380–2392. <https://doi.org/10.1021/acsami.5b11533>
- Koley P, Sakurai M, Takei T, Aono M (2016b) Facile fabrication of silk protein sericin-mediated hierarchical hydroxyapatite-based bio-hybrid architectures: excellent adsorption of toxic heavy metals and hazardous dye from wastewater. *RSC Adv* 6:86607–86616. <https://doi.org/10.1039/C6RA12818A>
- Kos M, Kahru A, Drobne D et al (2016) A case study to optimise and validate the brine shrimp *Artemia franciscana* immobilisation assay with silver nanoparticles: The role of harmonisation. *Environ Pollut* 213:173–183. <https://doi.org/10.1016/j.envpol.2016.02.015>
- Kubra KT, Salman MS, Hasan MN et al (2021) Utilizing an alternative composite material for effective copper(II) ion capturing from wastewater. *J Mol Liq* 336:116325. <https://doi.org/10.1016/j.molliq.2021.116325>
- Kushwaha A, Rani R, Patra JK (2020) Adsorption kinetics and molecular interactions of lead [Pb(II)] with natural clay and humic acid. *Int J Environ Sci Technol* 17:1325–1336. <https://doi.org/10.1007/s13762-019-02411-6>
- Le TH, Van HN, Sorgeloos P, Van Stappen G (2019) *Artemia* feeds: a review of brine shrimp production in the Mekong Delta. *Vietnam Rev Aquac* 11:1169–1175. <https://doi.org/10.1111/raq.12285>
- Li Y, Zhang P, Du Q et al (2011) Adsorption of fluoride from aqueous solution by graphene. *J Colloid Interface Sci* 363:348–354. <https://doi.org/10.1016/j.jcis.2011.07.032>
- Li Z, Wang L, Meng J et al (2018) Zeolite-supported nanoscale zero-valent iron: New findings on simultaneous adsorption of Cd(II), Pb(II), and As(III) in aqueous solution and soil. *J Hazard Mater* 344:1–11. <https://doi.org/10.1016/j.jhazmat.2017.09.036>
- Liang Y, Chen JQ, Mei J et al (2019) Characterization of Cu and Cd biosorption by *Pseudomonas* sp. strain DC-B3 isolated from metal mine soil. *Int J Environ Sci Technol* 16:4035–4046. <https://doi.org/10.1007/s13762-018-2011-5>
- Libralato G (2014) The case of *Artemia* spp. in nanocotoxicology. *Mar Environ Res* 101:38–43. <https://doi.org/10.1016/j.marenvres.2014.08.002>
- Liu B, Lv X, Meng X et al (2013) Removal of Pb(II) from aqueous solution using dithiocarbamate modified chitosan beads with Pb(II) as imprinted ions. *Chem Eng J* 220:412–419. <https://doi.org/10.1016/j.cej.2013.01.071>
- Liu Y, Xing R, Yang H et al (2020) Chitin extraction from shrimp (*Litopenaeus vannamei*) shells by successive two-step fermentation with *Lactobacillus rhamnoides* and *Bacillus amyloliquefaciens*. *Int J Biol Macromol* 148:424–433. <https://doi.org/10.1016/j.ijbiomac.2020.01.124>
- Luo X, Zeng J, Liu S, Zhang L (2015) An effective and recyclable adsorbent for the removal of heavy metal ions from aqueous system: Magnetic chitosan/cellulose microspheres. *Bioresour Technol* 194:403–406. <https://doi.org/10.1016/j.biortech.2015.07.044>
- MacRae TH (2016) Stress tolerance during diapause and quiescence of the brine shrimp, *Artemia*. *Cell Stress Chaperones* 21:9–18. <https://doi.org/10.1007/s12192-015-0635-7>
- Malik H, Qureshi UA, Muqet M et al (2018) Removal of lead from aqueous solution using polyacrylonitrile/magnetite nanofibers. *Environ Sci Pollut Res* 25:3557–3564. <https://doi.org/10.1007/s11356-017-0706-7>
- Mallampati R, Xuanjun L, Adin A, Valiyaveetil S (2015) Fruit Peels as Efficient Renewable Adsorbents for Removal of Dissolved Heavy Metals and Dyes from Water. *ACS Sustain Chem Eng* 3:1117–1124. <https://doi.org/10.1021/acsschemeng.5b00207>
- Meena AK, Mishra GK, Rai PK et al (2005) Removal of heavy metal ions from aqueous solutions using carbon aerogel as an adsorbent. *J Hazard Mater* 122:161–170. <https://doi.org/10.1016/j.jhazmat.2005.03.024>
- Meski S, Ziani S, Khireddine H (2010) Removal of Lead Ions by Hydroxyapatite Prepared from the Egg Shell. *J Chem Eng Data* 55:3923–3928. <https://doi.org/10.1021/je901070e>
- Rao GP, Lu C, Su F (2007) Sorption of divalent metal ions from aqueous solution by carbon nanotubes: A review. *Sep Purif Technol* 58:224–231. <https://doi.org/10.1016/j.seppur.2006.12.006>
- Saha GC, Hoque MIU, Miah MAM et al (2017) Biosorptive removal of lead from aqueous solutions onto Taro (*Colocasia esculenta*(L.) Schott) as a low cost bioadsorbent: Characterization, equilibria, kinetics and biosorption-mechanism studies. *J Environ Chem Eng* 5:2151–2162. <https://doi.org/10.1016/j.jece.2017.04.013>
- Sarode S, Upadhyay P, Khosa MA et al (2019) Overview of wastewater treatment methods with special focus on biopolymer chitin-chitosan. *Int J Biol Macromol* 121:1086–1100. <https://doi.org/10.1016/j.ijbiomac.2018.10.089>
- Sellaoui L, Franco DSP, Dotto GL et al (2017) Single and binary adsorption of cobalt and methylene blue on modified chitin: Application of the Hill and exclusive extended Hill models. *J Mol Liq* 233:543–550. <https://doi.org/10.1016/j.molliq.2016.10.079>
- Soares MAR, Marto S, Quina MJ et al (2016) Evaluation of Eggshell-Rich Compost as Biosorbent for Removal of Pb(II) from Aqueous Solutions. *Water, Air, Soil Pollut* 227:150. <https://doi.org/10.1007/s11270-016-2843-x>
- Song Y, Song X, Sun Q et al (2022) Efficient and sustainable phosphate removal from water by small-sized Al(OH)<sub>3</sub> nanocrystals confined in discarded *Artemia* Cyst-shell: Ultrahigh sorption capacity and rapid sequestration. *Sci Total Environ* 803:150087. <https://doi.org/10.1016/j.scitotenv.2021.150087>
- Sorgeloos P, Dhert P, Candreva P (2001) Use of the brine shrimp, *Artemia* spp., in marine fish larviculture. *Aquaculture* 200:147–159. [https://doi.org/10.1016/S0044-8486\(01\)00698-6](https://doi.org/10.1016/S0044-8486(01)00698-6)
- Sugumar V, Munuswamy N (2006) Ultrastructure of cyst shell and underlying membranes of three strains of the brine shrimp *Artemia* (Branchiopoda: Anostraca) from South India. *Microsc Res Tech* 69:957–963. <https://doi.org/10.1002/jemt.20371>
- Tolesa LD, Gupta BS, Lee M (2019) International Journal of Biological Macromolecules Chitin and chitosan production from shrimp shells using ammonium-based ionic liquids. *Int J Biol Macromol* 130:818–826. <https://doi.org/10.1016/j.ijbiomac.2019.03.018>
- Turkmen Koc SN, Kipcak AS, Moroydor Derun E, Tugrul N (2020) Removal of zinc from wastewater using orange, pineapple and pomegranate peels. *Int J Environ Sci Technol*. <https://doi.org/10.1007/s13762-020-03025-z>
- Velde K Van De, Kiekens P (2004) Structure analysis and degree of substitution of chitin, chitosan and dibutylchitin by FT-IR spectroscopy and solid state <sup>13</sup>C NMR. *58:409–416*. <https://doi.org/10.1016/j.carbpol.2004.08.004>
- Vieira RM, Vilela PB, Becegato VA, Paulino AT (2018) Chitosan-based hydrogel and chitosan/acid-activated montmorillonite composite hydrogel for the adsorption and removal of Pb+2 and Ni+2 ions accommodated in aqueous solutions. *J Environ Chem Eng* 6:2713–2723. <https://doi.org/10.1016/j.jece.2018.04.018>
- Wan S, He F, Wu J et al (2016) Rapid and highly selective removal of lead from water using graphene oxide-hydrated manganese oxide nanocomposites. *J Hazard Mater* 314:32–40. <https://doi.org/10.1016/j.jhazmat.2016.04.014>
- Wang B, Xia J, Mei L et al (2018) Highly Efficient and Rapid Lead(II) Scavenging by the Natural *Artemia* Cyst Shell with Unique Three-Dimensional Porous Structure and Strong Sorption Affinity. *ACS Sustain Chem Eng* 6:1343–1351. <https://doi.org/10.1021/acssuschemeng.7b03667>
- Wang J, Guo X (2020) Adsorption isotherm models: Classification, physical meaning, application and solving method. *Chemosphere* 258:127279. <https://doi.org/10.1016/j.chemosphere.2020.127279>
- Wang J, Zhuang S (2017) Removal of various pollutants from water and wastewater by modified chitosan adsorbents. *Crit Rev Environ*





- Sci Technol 47:2331–2386. <https://doi.org/10.1080/10643389.2017.1421845>
- Wang S-F, Sun S-C, Okazaki RK (2010) Comparative study on thermo-tolerance of *Artemia* resting eggs from Qinghai-Xizang Plateau, China. *Aquaculture* 307:141–149. <https://doi.org/10.1016/j.aquaculture.2010.07.009>
- Wang S, Ma M, Zhang Q, et al (2015) Efficient Phosphate Sequestration in Waters by The Unique Hierarchical 3D *Artemia* Egg Shell Supported Nano-Mg (OH)<sub>2</sub> Composite and Sequenced Potential Application in Slow Release Fertilizer Efficient Phosphate Sequestration in Waters by The Unique Hiera. <https://doi.org/10.1021/acssuschemeng.5b00594>
- WHO (2019) Exposure to Lead: A major public health concern (2019 revision). World Heal Organ
- Xu L, Wang J (2017) The application of graphene-based materials for the removal of heavy metals and radionuclides from water and wastewater. *Crit Rev Environ Sci Technol* 47:1042–1105. <https://doi.org/10.1080/10643389.2017.1342514>
- Yang H (2007) Characteristics of hemicellulose, cellulose and lignin pyrolysis. 86:1781–1788. <https://doi.org/10.1016/j.fuel.2006.12.013>
- Yılmaz EŞ, Öztürk Ş, Aslım B (2020) Effects of some heavy metals on thiol compounds in *Synechocystis* sp. isolates. *Int J Environ Sci Technol* 17:3013–3022. <https://doi.org/10.1007/s13762-020-02709-w>
- Zhang L, Zeng Y, Cheng Z (2016) Removal of heavy metal ions using chitosan and modified chitosan: A review. *J Mol Liq* 214:175–191. <https://doi.org/10.1016/j.molliq.2015.12.013>
- Zhang Q, Yang Q, Phanlavong P, et al (2017) Highly Efficient Lead(II) Sequestration Using Size-Controllable Polydopamine Microspheres with Superior Application Capability and Rapid Capture. <https://doi.org/10.1021/acssuschemeng.7b00129>
- Zhang Q, Zhang S, Zhao Z et al (2020) Highly effective lead (II) removal by sustainable alkaline activated  $\beta$ -lactoglobulin nanofibrils from whey protein. *J Clean Prod* 255:120297. <https://doi.org/10.1016/j.jclepro.2020.120297>
- Zhou D, Zhang L, Guo S (2005a) Mechanisms of lead biosorption on cellulose/chitin beads. *Water Res* 39:3755–3762. <https://doi.org/10.1016/j.watres.2005.06.033>
- Zhou D, Zhang L, Guo S (2005b) Mechanisms of Lead Biosorption on Cellulose / Chitin Beads 39:3755–3762. <https://doi.org/10.1016/j.watres.2005.06.033>
- Zia Z, Hartland A, Mucalo MR (2020) Use of low-cost biopolymers and biopolymeric composite systems for heavy metal removal from water. *Int J Environ Sci Technol* 17:4389–4406. <https://doi.org/10.1007/s13762-020-02764-3>

